Biomedical Optics EXPRESS

Stokes vector based polarization resolved second harmonic microscopy of starch granules

Nirmal Mazumder,[1] Jianjun Qiu,[1] Matthew R. Foreman,[2,3] Carlos Macías Romero,[2] Peter Török,[2] and Fu-Jen Kao[1,*]

[1]*Institute of Biophotonics, National Yang-Ming University, 155, Li-Nong St., Taipei 11221, Taiwan*
[2]*Blackett Laboratory, Department of Physics, Imperial College London, Prince Consort Road, London SW7 2BZ, UK*
[3]*Max Planck Institute for the Science of Light, Günter-Scharowsky-Straße 1, 91058 Erlangen, Germany*
**fjkao@ym.edu.tw*

Abstract: We report on the measurement and analysis of the polarization state of second harmonic signals generated by starch granules, using a four-channel photon counting based Stokes-polarimeter. Various polarization parameters, such as the degree of polarization (DOP), the degree of linear polarization (DOLP), the degree of circular polarization (DOCP), and anisotropy are extracted from the 2D second harmonic Stokes images of starch granules. The concentric shell structure of a starch granule forms a natural photonic crystal structure. By integration over all the solid angle, it will allow very similar SHG quantum efficiency regardless of the angle or the states of incident polarization. Given type I phase matching and the concentric shell structure of a starch granule, one can easily infer the polarization states of the input beam from the resulting SH micrograph.

OCIS codes: (180.4315) Nonlinear microscopy; (120.5410) Polarimetry; (320.0320) Ultrafast optics; (120.0120) Instrumentation, measurement, and metrology; (160.1435) Biomaterials.

References and links

1. P. J. Campagnola and L. M. Loew, "Second-harmonic imaging microscopy for visualizing biomolecular arrays in cells, tissues and organisms," Nat. Biotechnol. **21**(11), 1356–1360 (2003).
2. W. Denk, J. H. Strickler, and W. W. Webb, "Two-photon laser scanning fluorescence microscopy," Science **248**(4951), 73–76 (1990).
3. F. Lu, W. Zheng, and Z. Huang, "Heterodyne polarization coherent anti-Stokes Raman scattering microscopy," Appl. Phys. Lett. **92**(12), 123901 (2008).
4. S. V. Plotnikov, A. C. Millard, P. J. Campagnola, and W. A. Mohler, "Characterization of the myosin-based source for second-harmonic generation from muscle sarcomeres," Biophys. J. **90**(2), 693–703 (2006).
5. P. J. Campagnola, "Second harmonic generation imaging microscopy: applications to diseases diagnostics," Anal. Chem. **83**(9), 3224–3231 (2011).
6. X. Chen, O. Nadiarynkh, S. Plotnikov, and P. J. Campagnola, "Second harmonic generation microscopy for quantitative analysis of collagen fibrillar structure," Nat. Protoc. **7**(4), 654–669 (2012).
7. R. W. Boyd, *Nonlinear Optics* (Academic Press, 1992).
8. S. Psilodimitrakopoulos, S. I. C. O. Santos, I. Amat-Roldan, A. K. N. Thayil, D. Artigas, and P. Loza-Alvarez, "In vivo, pixel-resolution mapping of thick filaments' orientation in nonfibrilar muscle using polarization-sensitive second harmonic generation microscopy," J. Biomed. Opt. **14**(1), 014001 (2009).
9. G. Cox, N. Moreno, and J. Feijó, "Second-harmonic imaging of plant polysaccharides," J. Biomed. Opt. **10**(2), 024013 (2005).
10. A. D. Slepkov, A. Ridsdale, A. F. Pegoraro, D. J. Moffatt, and A. Stolow, "Multimodal CARS microscopy of structured carbohydrate biopolymers," Biomed. Opt. Express **1**(5), 1347–1357 (2010).
11. Z. Y. Zhuo, C. S. Liao, C. H. Huang, J. Y. Yu, Y. Y. Tzeng, W. Lo, C. Y. Dong, H. C. Chui, Y. C. Huang, H. M. Lai, and S. W. Chu, "Second harmonic generation imaging—a new method for unraveling molecular information of starch," J. Struct. Biol. **171**(1), 88–94 (2010).
12. S. Psilodimitrakopoulos, I. Amat-Roldan, P. Loza-Alvarez, and D. Artigas, "Estimating the helical pitch angle of amylopectin in starch using polarization second harmonic generation microscopy," J. Opt. **12**(8), 084007 (2010).
13. S. Psilodimitrakopoulos, I. Amat-Roldan, P. Loza-Alvarez, and D. Artigas, "Effect of molecular organization on the image histograms of polarization SHG microscopy," Biomed. Opt. Express **3**(10), 2681–2693 (2012).
14. R. L. Whistler, J. N. Bemiller, and E. F. Parschall, *Starch: Chemistry and Technology* (Academic Press, 1984), pp. 183–247.

#182802 - $15.00 USD Received 7 Jan 2013; revised 23 Feb 2013; accepted 23 Feb 2013; published 11 Mar 2013

15. D. J. Gallant, B. Bouchet, A. Buléon, and S. Pérez, "Physical characteristics of starch granules and susceptibility to enzymatic degradation," Eur. J. Clin. Nutr. **46**(Suppl 2), S3–S16 (1992).
16. D. J. Gallant, B. Bouchet, and P. M. Baldwin, "Microscopy of starch: evidence of a new level of granule organization," Carbohydr. Polym. **32**(3-4), 177–191 (1997).
17. G. T. Oostergetel and E. F. J. van Bruggen, "On the origin of a low angle spacing in starch," Starch **41**(9), 331–335 (1989).
18. G. Mizutani, Y. Sonoda, H. Sano, M. Sakamoto, T. Takahashi, and S. Ushioda, "Detection of starch granules in a living plant by optical second harmonic microscopy," J. Lumin. **87-89**, 824–826 (2000).
19. R. Carriles, K. E. Sheetz, E. E. Hoover, J. A. Squier, and V. Barzda, "Simultaneous multifocal, multiphoton, photon counting microscopy," Opt. Express **16**(14), 10364–10371 (2008).
20. K. N. Anisha Thayil, E. J. Gualda, S. Psilodimitrakopoulos, I. G. Cormack, I. Amat-Roldán, M. Mathew, D. Artigas, and P. Loza-Alvarez, "Starch-based backwards SHG for in situ MEFISTO pulse characterization in multiphoton microscopy," J. Microsc. **230**(1), 70–75 (2008).
21. M. Wang, K. M. Reiser, and A. Knoesen, "Spectral moment invariant analysis of disorder in polarization-modulated second-harmonic-generation images obtained from collagen assemblies," J. Opt. Soc. Am. A **24**(11), 3573–3586 (2007).
22. M. R. Foreman, C. Macias Romero, and P. Török, "A priori information and optimisation in polarimetry," Opt. Express **16**(19), 15212–15227 (2008).
23. R. M. A. Azzam, "Arrangement of four photodetectors for measuring the state of polarization of light," Opt. Lett. **10**(7), 309–311 (1985).
24. P. A. Letnes, I. S. Nerbø, L. M. S. Aas, P. G. Ellingsen, and M. Kildemo, "Fast and optimal broad-band Stokes/Mueller polarimeter design by the use of a genetic algorithm," Opt. Express **18**(22), 23095–23103 (2010).
25. C. W. Sun, C. C. Yang, and Y. W. Kiang, "Optical imaging based on time-resolved Stokes vectors in filamentous tissues," Appl. Opt. **42**(4), 750–754 (2003).
26. V. Sankaran, Jr., J. T. Walsh, Jr., and D. J. Maitland, "Comparative study of polarized light propagation in biologic tissues," J. Biomed. Opt. **7**(3), 300–306 (2002).
27. V. K. Valev, A. V. Silhanek, N. Smisdom, B. De Clercq, W. Gillijns, O. A. Aktsipetrov, M. Ameloot, V. V. Moshchalkov, and T. Verbiest, "Linearly polarized second harmonic generation microscopy reveals chirality," Opt. Express **18**(8), 8286–8293 (2010).
28. T. Verbiest, M. Kauranen, J. J. Maki, M. N. Teerenstra, A. J. Schouten, R. J. M. Nolte, and A. Persoons, "Linearly polarized probes of surface chirality," J. Chem. Phys. **103**(18), 8296–8298 (1995).
29. N. Mazumder, J. Qiu, M. R. Foreman, C. M. Romero, C.-W. Hu, H.-R. Tsai, P. Török, and F.-J. Kao, "Polarization-resolved second harmonic generation microscopy with a four-channel Stokes-polarimeter," Opt. Express **20**(13), 14090–14099 (2012).
30. E. Collett, *Polarized Light: Fundamentals and Applications* (Marcel Dekker, 1993).
31. J. G. Webster, "Polarization measurement," in *The Measurement, Instrumentation and Sensors Handbook* (CRC Press, 1998), Chap. 60.
32. J. Qiu (Modern Optics Laboratory, National Yang-Ming University, 155 Li-Nong St., Taipei 112, Taiwan) and N. Mazumder are preparing a manuscript to be called "Stokes vector formalism based nonlinear optical microscopy."
33. A. Buléon, P. Colonna, V. Planchot, and S. Ball, "Starch granules: structure and biosynthesis," Int. J. Biol. Macromol. **23**(2), 85–112 (1998).
34. T. A. Waigh, K. L. Kato, A. M. Donald, M. J. Gidley, C. J. Clarke, and C. Riekel, "Side-chain liquid-crystalline model for starch," Starch **52**(12), 450–460 (2000).

1. Introduction

Nonlinear microscopy techniques exploiting, for example, second and third harmonic generation (SHG and THG) [1], two-photon excitation fluorescence (TPEF) [2] and coherent anti-Stokes Raman scattering (CARS) [3] are widely used in cellular and tissue imaging because they allow high molecular contrast, therefore enabling characterization of subcellular details. Much effort has been made, for example, in SHG microscopy of non-centrosymmetric biological media and structures, such as collagen and myosin [4–6], due to the strong structural dependence of SHG [1,7]. Strong SHG signals are also known to arise in plant samples, due to semi-crystalline polysaccharides, such as cellulose and starch, which are present [8,9], however detailed characterization of SHG signals originating from these bio-molecules has not yet been fully pursued. Combination of SHG and CARS microscopy has only recently, for instance, been used to investigate the internal structural and chemical information of starch granules [10]. It has, however, been demonstrated that there is a significant relationship between polarization-resolved SHG signals and the crystalline structure of different types of starch grains [11–13]. Specifically it is noted that the second

#182802 - $15.00 USD Received 7 Jan 2013; revised 23 Feb 2013; accepted 23 Feb 2013; published 11 Mar 2013

harmonic (SH) signal contrast is dependent on the incident polarization state, hence providing an interesting means to probe molecular orientation and disorder [6].

Starch is a glucose polymer often found in plants in the form of grains. These grains are water insoluble macroscopic complex networks of amylose and amylopectin [14], organized in alternating concentric 120–400 nm thick amorphous and semi-crystalline domains, known as growth rings [10,15]. The concentric shell structure of a starch granule hence forms a natural photonic crystal structure. The organization of the semi-crystalline shells has been widely studied by scanning electron microscopy of thin sections of granules [16,17], nevertheless, detailed knowledge regarding the structure, organization and arrangement of lamellae is still limited. The crystalline layers consist of ordered regions comprising double helical structures formed by short amylopectin branches. The amylopectin chains in the crystalline layers are strongly anisotropically aligned within the focal volume of the laser and thus yield a strong second-order nonlinear optical response [9,18]. Importantly, it should be noted that SHG microscopy usually relies on Type I phase matching, that is $h\nu_{\omega,\ \text{ordinary}} + h\nu_{\omega,\ \text{ordinary}} \rightarrow h\nu_{2\omega,\ \text{extraordinary},}$ for the SH signal. Unlike nonlinear optical crystals, such as KDP, LBO, etc., the concentric shell (or ring) structure of starch granules implies that phase matching is more easily satisfied. Given type I phase matching and the concentric shell structure of a starch granule, one can easily infer the polarization states of the input beam from the resulting SH micrograph as will be seen below.

The utility of SHG microscopy for the study of starch grains is a current topic of research interest [13,19,20]. The implementation of polarization measurements and SHG imaging of starch grains provide complimentary information about micro-domains [11]. Specifically polarization-resolved SHG microscopy can provide information about the orientation and degree of structural organization inside biological samples using the anisotropy parameter and other signal analysis methods [13,21].Since the focal volume of the microscope objective is much smaller than the granules in the focal plane, the SHG intensity in each pixel depends on the net orientation of the electric dipoles within the illumination focal spot and the input polarization of the laser beam. We have developed a four-channel Stokes-polarimeter based on a pixel by pixel image analysis, capable of characterizing the polarization response of starch spatially. The polarization state of the SHG signal after interaction of the light with the amylopectin is characterized by the Stokes parameters, which can be inferred from the measured intensities in each polarimeter channel. Stokes polarimetry requires combination of a polarization state generator (PSG), a sample and a polarization state analyzer (PSA) to deduce the Stokes parameters [22–24]. Most Stokes polarimetry studies have focused on using linear optical process on a sample and measuring the degree of polarization of the light in transmission mode [25,26].

It is reported that chirality can be detected by linearly polarized light generated via a second harmonic or sum-frequency generation process and may arise entirely in the electric-dipole approximation [27,28]. SHG efficiency from chiral molecules has a strong dependence upon the handedness circularly polarized excitation beam.

In this work, we describe the application of a four-channel photon counting based Stokes polarimetric and SHG imaging technique to determine the complete polarization state of SH light and to differentiate macroscopic structures of starch granules. By varying the incident polarization and detecting the SH signal originating from a single plane, a differential measurement can be made. Again, we observed that signals from starch granules reflect the polarization states of the incident excitation beams due to their concentric shell like structure. We also report on characterization of the polarization properties of the molecular structure of starch, by deriving various polarization parameters from the measured Stokes vectors, such as the degree of linear and circular polarization.

#182802 - $15.00 USD Received 7 Jan 2013; revised 23 Feb 2013; accepted 23 Feb 2013; published 11 Mar 2013

2. Materials and methods

2.1 Polarization imaging system

The experimental arrangement of our SHG imaging system, used to measure the polarization states of the SHG signal, is described in detail in [29]. A femtosecond Ti:Sapphire (Coherent Mira Optima 900-F) laser oscillator, with central wavelength of 800 nm, a full width at half maximum (FWHM) spectral width of 15 nm pulses with duration of ~100 fs, average power ~550 mW, and repetition rate ~76 MHz, was used as the excitation light source. Samples were mounted upside-down on an XYZ stage and scanned with a laser scanning unit (Olympus, FV300). The measured signals were analyzed by means of a polarization state analyzer (PSA), specifically, a four-channel Stokes-polarimeter (see Fig. 1). In the four-channel Stokes-polarimeter imaging configuration, an objective lens (UPlanFLN40X/N.A. 1.3 oil, Olympus Corp., Japan) and a long-working distance 0.5 N.A. condenser provide excitation and SHG signal collection, respectively. A band pass filter of 400 ± 40 nm (Edmund Optics Inc. Barrington, New Jersey) was also inserted into the SHG emission path. The central SHG wavelength was verified using a fiber optic spectrometer (QE 65000, Ocean Optics) to be 400 nm. Stokes images, denoted '$\mathbf{S}_{out}$', were determined from four distinct polarization resolved SH intensity images, measured using a 256 × 256 pixel array, corresponding to 50 × 50 μm scanning area, by means of the algorithm detailed in Section 2.2. A pixel dwell time of 8μs was used and the light was collected by PMTs through standard multimode fibers (FT1500EMT, 1.5 mm core diameter, 0.39 N.A., Thorlabs).

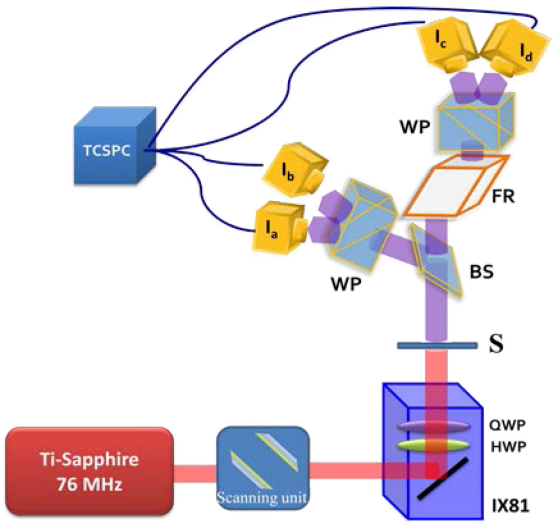

Fig. 1. Schematic diagram of our polarization-resolved SHG microscope with four-channel Stokes-polarimeter module. IX81: The Olympus inverted optical microscope, HWP: Half wave-plate, QWP: Quarter wave-plate, S: Sample, BS: beam splitter, FR: Fresnel Rhomb, WP: Wollaston Prism, Ia, Ib, Ic, Id: photo-multiplier tubes (PMTs). TCSPC: Time Correlated Single Photon Counter.

The PMTs were connected to time-correlated single photon counting (TCSPC) electronics for improving sensitivity and signal-to-noise ratio. The measured intensity signals were relayed through a four-channel router (PHR800, PicoQuant GmbH, Berlin, Germany). Data collection and primary analysis was performed using a commercial software package (SymPhoTime, PicoQuant GmbH, Berlin, Germany).

#182802 - $15.00 USD Received 7 Jan 2013; revised 23 Feb 2013; accepted 23 Feb 2013; published 11 Mar 2013

2.2 Image processing and algorithms

Stokes parameters, denoted $[S_0, S_1, S_2, S_3]$, give a convenient and complete description of the polarization state of light, and were thus used to characterize the polarization state of detected SH signals. Physically, S_0 represents the total intensity of the emitted signal, S_1 is the intensity difference in the intensities between horizontal and vertical linear polarization states at 0° and 90°, S_2 is the intensity difference between linear polarization states at 45° and −45°, and S_3 is the difference in intensities between right (RCP) and left-handed (LCP) circular polarization states, respectively [30]. To determine the Stokes parameters, $\mathbf{S}_{out} = [S_0, S_1, S_2, S_3]$, of the SH signal, the measured intensity images were analyzed on a pixel by pixel basis. Specifically, the four SHG signal intensities detected by corresponding pixels in the TCSPC electronics of each measurement arm of the Stokes-polarimeter, were first stacked to form a vector $\mathbf{I} = [I_a I_b I_c I_d]^t$ (counts per msec). Importantly, the intensity vector, **I**, can be expressed as the product of a 4 × 4 instrument matrix 'A_{4x4}' describing the Stokes-polarimeter and the 4 × 1 Stokes vector, $\mathbf{S}_{out}$, of the SH signal, i.e. $\mathbf{I} = A_{4\times4}\mathbf{S}_{out}$. Accordingly, the output Stokes vector $\mathbf{S}_{out}$ was therefore determined using the inverse relationship $\mathbf{S}_{out} = (A_{4\times4})^{-1}\mathbf{I}$. This equation highlights the importance of the instrument matrix with regards to correct sample analysis.

Using the Stokes parameters, further physically important parameters, such as the degree of polarization (DOP), the degree of linear polarization (DOLP), the degree of circular polarization (DOCP) and anisotropy (*r*) of the SH signal at each pixel of the scanning area can also calculated [29,31]. In this regard, we have developed a series of specialized routines in MATLAB (MathWorks, R2009b) to automate reconstruction of the 2D intensity images, the corresponding Stokes vector and related parameter distributions, from the acquired TCSPC data.

2.3 Sample preparation

The different polarization properties of SHG signals were obtained from starch granules using our Stokes-polarimeter setup. By varying the polarization states of the incident beam and detecting the change of different polarization components of the SH signal after the sample, we reconstructed 2D SHG Stokes images of starch granules. The polarization-resolved SH images were obtained from potato starch suspended in aqueous solution. The starch granules were extracted from home-grown potatoes by suspending freshly-cut pieces in tap-water at room-temperature for one hour. The starch grains rapidly settle to the bottom of the beaker and were transferred to a sample vial using a pipette, and subsequently washed, several times, in clean tap water. A drop of a dilute starch-water suspension was then placed on a coverslip and the water allowed to evaporate in a flow-hood [10]. The starch grain samples then adhered to the coverslip, were re-wetted with the surrounding medium and covered with a further coverslip. The samples were mounted upside-down in the microscope stage.

2.4 Calibration

The Stokes vector of SH signals from a sample can be determined accurately if the instrument matrix 'A_{4x4}' of the polarimeter is known. In reality, the instrument matrix is however determined by system calibration, by inputting a set of known input polarization states into the polarimeter and measuring the output intensities. To avoid dispersion effects in the polarimeter, we inserted a polarization state generator (PSG) after the sample stage, comprised of KDP micro-crystals (SIGMA, Germany) sandwiched between two cover glass slips and immersed in oil, for optimal index matching. By focusing the 800 nm pump laser onto the KDP sample, a 400 nm SHG signal is produced. The generated SH light is collimated by the condenser lens operating in transmission mode and relayed to the PSG, as described in the Materials and Methods of our previous work [29], to generate 0°, 90°, 45° and RC polarization states. The PSG is removed once the polarimeter is calibrated. Figure 2 shows the normalized Stokes parameters of the SH beams, after the PSG, that were input into the

#182802 - $15.00 USD Received 7 Jan 2013; revised 23 Feb 2013; accepted 23 Feb 2013; published 11 Mar 2013

polarimeter. S_0 is normalized to its maximum value and S_1, S_2, S_3 are normalized to S_0 in a pixel-wise manner. It is evident from Fig. 2 that the values of the Stokes parameters of the given polarization state are close to the theoretical values.

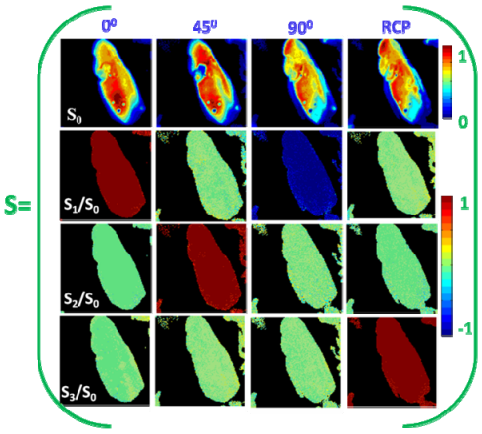

Fig. 2. Shows the reconstructed 2D Stokes images for input polarization states correspond to 0°, 45°, 90° linear, and RC polarization, respectively. The color scale shows the values of each parameter increasing from blue to red. The theoretical values of S_0, S_1/S_0, S_2/S_0 and S_3/S_0 at 0°, 45°, 90°, RCP are [1 1 0 0], [1 0 1 0], [1 –1 0 0] and [1 0 0 1], respectively.

We optimized our four-channel Stokes-polarimeter for operation at 400 nm, by minimizing the condition number of the instrument matrix $(A_{4x4})^{-1}$, implying that propagation of errors from the measured intensities to the determined Stokes parameters was minimal [22]. In this work, we typically tuned the PSA to achieve a condition number of the instrument matrix of 3.0. The performance and accuracy of the four-channel Stokes-polarimeter are discussed in detail in [32].

3. Results and discussion

3.1 Illumination dependence of the SHG intensity from starch

It is known that SHG signal strength depends on the geometrical characteristics and the relative path differences between SHG active molecules within the sample [33]. To investigate this phenomenon further, we acquired a large variety of SH intensity patterns, by varying the polarization state of the incident laser light and detecting different polarization components of the SH signal via our PSA. Figure 3(a) and Fig. 3(b) show, for example, the reconstructed 2D Stokes images derived from SH signals originating from starch granules when illuminated with horizontally and vertically polarized light respectively. From the Stokes parameters, it is evident that an excitation pulse of linearly polarized light (which can equivalently be considered as an equal superposition of right and left circular polarized light) is transformed into right or left elliptically polarized light. The effect of different input polarization states is thus evident from the 2D reconstructed Stokes images of SH signal. Polarization light microscopy has been used to show that starch granules exhibit positive birefringence and theoretically it is predicted that crystallinity in starch granules is aligned in a radial direction [16,34]. Although, optical methods using birefringence and interference have been used to determine the macromolecular orientation in starch, to date a full determination of the polarization state of the output signals has not been reported. We demonstrate here that this output polarization directly reflects the molecular symmetry of starch granules.

#182802 - $15.00 USD Received 7 Jan 2013; revised 23 Feb 2013; accepted 23 Feb 2013; published 11 Mar 2013

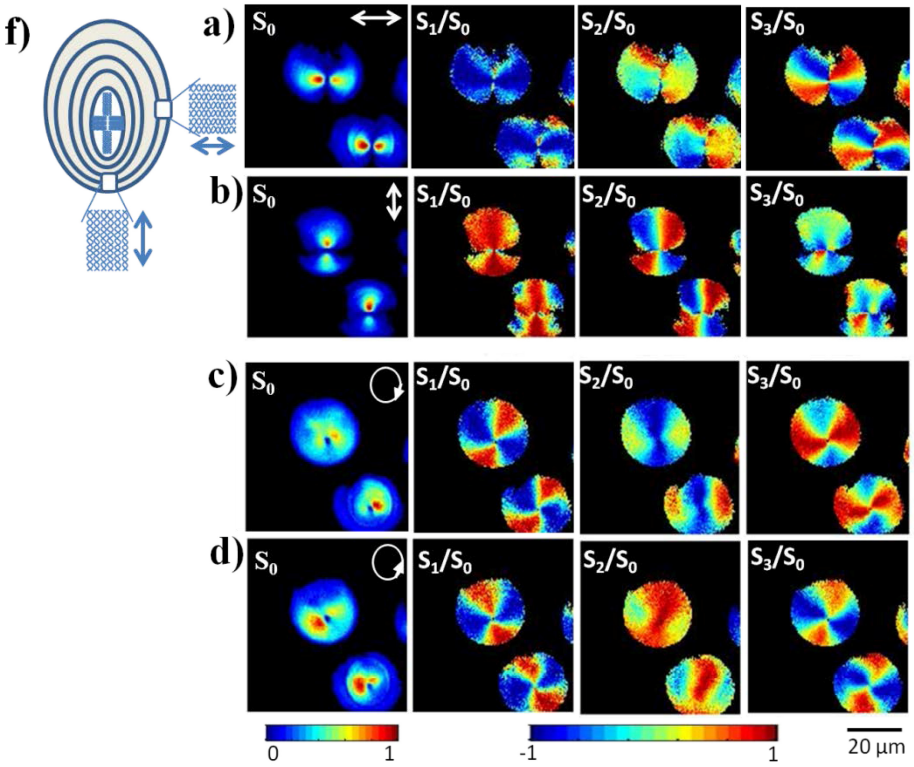

Fig. 3. Experimental reconstructed 2D Stokes images of the SHG response from starch granules for (a) horizontally, (b) vertically, (c) right and (d) left circularly polarized illumination, respectively. White arrows in the leftmost images indicate the direction of polarization. The color scale shows the value of each Stokes parameter increasing from blue to red. A schematic model of a starch granule is shown in (f).

As shown in Fig. 3(a) and Fig. 3(b), the SHG intensity images (S_0) of the same sample area and depth exhibit a two-lobe structure, oriented parallel to the linearly excited polarization directions. For a fixed linear laser excitation polarization, the SHG intensity is a function of $\cos^2\theta$, where θ is the angle between the state of (linear) polarization and the net orientation of dipoles within the excitation region [6]. For example, the SHG intensity is minima when the laser polarization and SHG radiating dipoles are orthogonally oriented [4]. Accordingly the two lobe structure can be attributed to the radial arrangement of the SHG active crystals i.e. amylopectin in the starch granules. Therefore, it is also seen that lobe orientation in the S_0intensity distribution mirrors the polarization state of the input beam. From the reconstructed 2D Stokes images, it is also observed that orthogonally polarized illuminations can generate different polarization states from different positions within a single starch granule. This is a consequence of chirality and anisotropy of the starch granules.

Figure 3(c) and Fig. 3(d) show the SHG images obtained from the same area as those shown in Fig. 3(a) and Fig. 3(b), albeit using a right and left circularly polarized illumination, respectively. Figure 3(c) and Fig. 3(d) demonstrate that circularly polarized light can excite all amylopectin molecules in the starch granules. Right and left circularly polarized light, however, is scattered by amylopectin molecules differently and is transformed into left or right elliptically polarized light depending on the handedness and absolute orientation of the amylopectin molecules. This behavior is particularly evident when considering the degree of circular polarization, as is discussed in the next section. Finally, it is worth noting that the hilum located at the centre of the starch granule (see Fig. 3(f)), is a centrosymmetric structure,

#182802 - $15.00 USD Received 7 Jan 2013; revised 23 Feb 2013; accepted 23 Feb 2013; published 11 Mar 2013

and thus gives rise to a dark spot in the Stokes images, when excited with both linearly and circularly polarized light. At other positions in the starch granule, however, differences in the polarization states of the SHG signals are clearly distinguishable, upon excitation with differently polarized illuminations.

3.2 Polarization properties of SHG signal from starch granule

As shown in the previous section, the SH yield from amylopectin molecules in starch granules has a strong polarization dependence (see also [12,20]). The unique advantage of SHG microscopy in combination with a four-channel Stokes-polarimeter, is the capability to extract the complete polarization state of the SH signal, from which additional molecular orientation information can be obtained, via further processing of the obtained Stokes parameters. Second-order effects are, in particular, very sensitive to the structural symmetry of the samples; such that the anisotropic and concentric shell structure of starch granules gives rise to a unique polarization dependent behavior of the SH signal. Figure 4, for instance, shows the spatial variation in the DOP, DOLP, DOCP and anisotropy, *r,* as was derived from SHG light obtained from starch granules upon illumination with different polarization states. Since these polarization parameters are related to the alignment of dipoles within the focal volume, Fig. 4 highlights the different morphologies of the crystallites present within a starch granule. These polarization-resolved SHG images were obtained without relying on any sample alignment or analyzer rotation before the detector.

As shown in Fig. 4, the DOP of the SH signal from starch is approximately unity, indicating that the SH signal from starch granules is predominantly fully polarized regardless of the illuminating polarization state. Physically, this fact demonstrates that the crystalline layer of amylopectin branches is well ordered. The DOLP distributions shown in Figs. 4(a) and 4(b), furthermore, depict the degree of crystalline alignment of molecules parallel in the horizontal and vertical directions respectively. The DOLP values for both horizontally and vertically polarized excitation is seen to peak at approximately unity and to vary sinusoidally with angle, again indicating a good radial alignment of the crystallites in the starch granules. Linearly polarized light interacting with the amylopectin molecules will, however, also undergo optical rotation by virtue of circular birefringence of the starch granules.

#182802 - $15.00 USD Received 7 Jan 2013; revised 23 Feb 2013; accepted 23 Feb 2013; published 11 Mar 2013

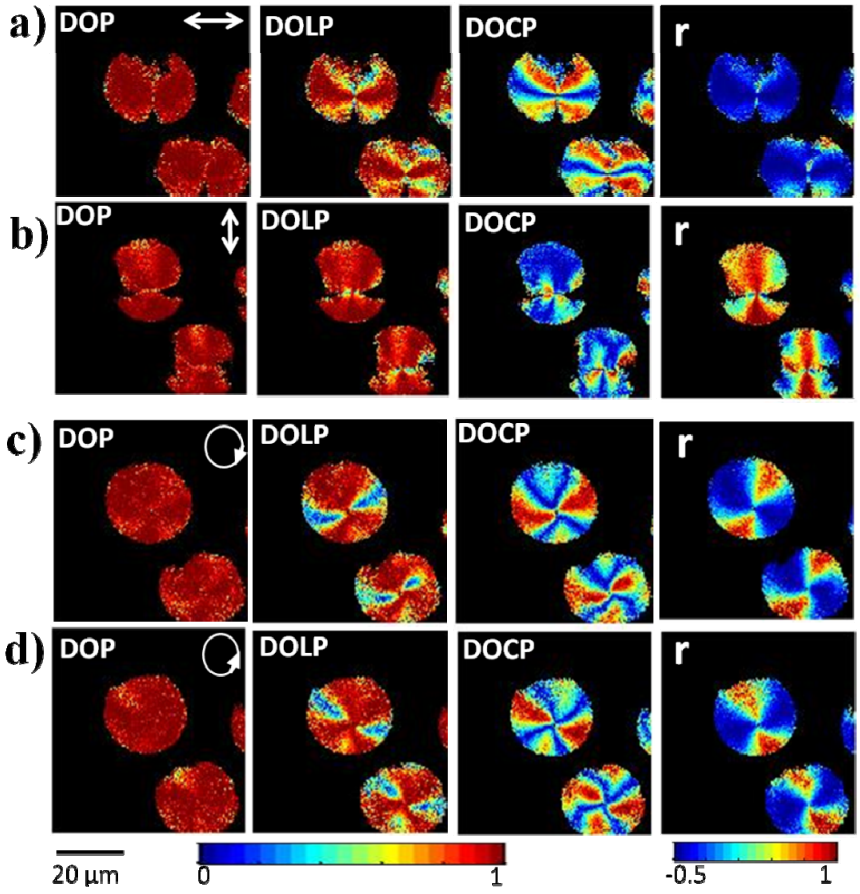

Fig. 4. Experimental polarization-resolved 2D reconstructed DOP, DOLP, DOCP and polarization anisotropy images of SHG response from starch granule for the; (a) horizontal, (b) vertical, (c) right and (d) left circularly polarized polarization respectively. The direction of polarization is indicated by a white arrow in the images. The color scale shows the values of each parameter increases from blue to red.

Similarly to above, Fig. 4(c) and Fig. 4(d), consider excitation with circularly polarized light. The corresponding DOP images show more homogeneity than for linearly polarized illumination, whilst the DOLP varied from 1 to 0. It should be noted that the strong SH signal arises because the fraction of different handed amylopectin molecules is unequal, in turn producing a non-centrosymmetric structure [29].The degree of circular birefringence of the SH signal is therefore expected to give information on the distribution of specific amylopectin molecules.

Ellipticity of the SH signal can, however, be quantified by the DOCP, defined as the fraction of the difference in intensities in left and right circularly polarized states to the total intensity. For linearly polarized excitation, the DOCP values varied in different regions as shown in Fig. 4. For horizontal and vertically polarized illumination, the DOCP is zero along the direction of excitation polarization, whereas the DOLP value is approximately 1 from the same regions. We note that the higher the value of DOLP, the lower the value of DOCP is, i.e. molecules are more arranged in a radial direction. The reverse relationship between the DOLP and the DOCP is seen when the starch granule is illuminated with circularly polarized light (Figs. 4(c) and 4(d)).The DOLP and DOCP distributions hence demonstrate that there exists components of both linearly and circularly polarized light in the SH signal. In particular, birefringence of starch granules gives rise to a variation of the relative phase between field

#182802 - $15.00 USD Received 7 Jan 2013; revised 23 Feb 2013; accepted 23 Feb 2013; published 11 Mar 2013

components [33] with position, which hence transforms an incoming polarized state. Depending on the sample depth, the resulting polarization state can vary between being fully linearly to circularly polarized light. When a circularly polarized illumination is used, the SHG intensity depends strikingly on the helical structure of the amylopectin molecule. Consequently, right and left circularly polarized light produce an asymmetric behavior of the SHG signal intensities generated from starch molecules. The concentric shell like structure in starch granules is seen to affect the SH polarization, resulting in a polarization shift away from both the fundamental and SH signal produced by the sample. This shift is clearly visible in the DOCP image and the SH signal is a mixture of both linearly and circularly polarized light. In this study, with the help of Stokes parameters we have hence shown that linearly polarized can be used to detect the handedness of helical materials.

The effect of birefringence on the SHG signal was also explored via anisotropy measurements, which confirm the strong differences from different areas of starch granule. The SHG anisotropy value (r) varies between −0.5 to 1, where $r = 0$ represents an arrangement of molecules (e.g. random), such that the parallel and perpendicular polarized components of the SHG intensity are equal. In contrast $r = 1$ corresponds to alignment of all molecular dipoles relative to the incident laser polarization. SHG polarization anisotropy furthermore provides additional information on the amylopectin distribution within a starch granule, since the SHG signal anisotropy is related to the alignment of molecular dipoles within the focal volumes [6,13]. Figure 4 shows the acquired polarization anisotropy (r) images of starch granules under differing illumination polarization states. For a horizontally polarized laser light, the anisotropy value has a minimum of approximately −0.5. Furthermore, for a vertically polarized illumination r peaks at approximately unity. In both cases there is an angular variation, in a similar manner to the S_1 images, indicating that amylopectin molecules are arranged in a radial manner. The anisotropy images thus reveal that starch granules are highly anisotropic, as would be expected based on the known pitches of distinct helices within the coil structure of amylopectin [6]. This suggests that starch granules possess cylindrical symmetry.

4. Conclusion

In this work, we developed a model Stokes vector based four-channel polarimeter integrated within a SHG microscope. Stokes vector based polarization measurements were performed in the forward direction for characterization of molecular structure and orientation of starch granules in a rapid manner. This technique was shown to yield the polarization states of SHG signals, as quantified by the Stokes parameters, for a fixed input polarization state. Furthermore, starch granules were shown to exhibit polarization distributions reflecting that of the input polarization, due to the radial distribution of amylopectin molecules. The DOLP and DOCP of SH signals were calculated and analyzed, further elucidating structural properties of individual starch granules. Finally, we presented a technique to observe type I phase matching and concentric shell like structure in starch granules through four-channel Stokes polarimeter. In conclusion, starch granules were extensively analyzed to demonstrate the validity, and potential, of 2D polarization resolved SHG microscopy.

Acknowledgments

We appreciate greatly fruitful discussions with Prof. Tsu-Wei Nee regarding implantation of Stokes vector based methods. The authors would also like to thank the National Science Council, Taiwan (NSC99-2627-M-010-002, NSC98-2627-M-010-006, NSC97-2112-M-010-002-MY3, and NSC98-2112-M-010-001-MY3) for their generous support of the reported work.

#182802 - $15.00 USD Received 7 Jan 2013; revised 23 Feb 2013; accepted 23 Feb 2013; published 11 Mar 2013